

# Study on Stress Zoning Characteristics and Rock Burst Prevention and Control of Gob-Side Coal Body Based on Microseismic and Numerical Simulation

Shijia Liu\*

School of Resources and Environment, Henan Polytechnic University, Jiaozuo 454000, China

\*Corresponding Author: Shijia Liu

## ABSTRACT

Rock burst is a typical dynamic disaster in coal mining, and its occurrence is closely related to the distribution of mining-induced stress. Taking the N2107 working face of Yuwu Coal Mine as the research object, this paper systematically studies the stress distribution and evolution law of the gob-side coal body during the retreat mining process by comprehensively applying theoretical analysis, in-situ stress monitoring, microseismic data inversion, and FLAC3D numerical simulation. The results show that under the influence of mining activities, the gob-side coal body can be divided into three typical zones: the decompression zone, the stress concentration zone, and the original stress zone. The peak of the stress concentration zone is located approximately 150 m from the gob-side of the working face, and the range of the decompression zone is about 35 m. The microseismic b-value inversion results are consistent with the conclusions of stress monitoring and numerical simulation, verifying the reliability of the stress zoning. Based on the characteristics of stress evolution, rock burst prevention measures are proposed, including implementing pressure-relief boreholes in the stress concentration zone, optimizing support parameters in the decompression zone, and combining real-time microseismic b-value monitoring for risk early warning. This study provides theoretical basis and technical support for safe and efficient mining in deep coal mines.

## KEYWORDS

Gob-side coal body; Mining-induced stress distribution; Microseismic; Rock burst.

## 1. INTRODUCTION

Rock burst is one of the common dynamic disasters in coal mining, which seriously restricts the safe and efficient extraction of coal resources in China. As one of the main controlling factors of rock burst occurrence, stress is the key factor determining whether a rock burst can occur and its intensity. During the retreat mining process of a working face, the original stress state of the coal seam is destroyed, causing the redistribution of stress in the surrounding coal body of the stope[1-3]. The coal body adjacent to the goaf is in a decompressed state, reducing the probability of rock burst accidents. Therefore, mastering the stress distribution and variation law of the coal body on the goaf side of the working face is of important guiding significance for evaluating the outburst hazard of the gob-side entry, reasonably designing underground mining and excavation schemes, and preventing rock burst accidents[4].

Researchers at home and abroad have carried out extensive research on the stress variation of the coal body around the stope. Academician Qian Minggao et al. explained the stress manifestation law of the stope by establishing the "masonry beam" bearing structure mechanical model, and found that there exist decompression zones, pressurization zones, and stable pressure zones around the stope[5-

8]. Xue Cheng et al. determined the advanced stress distribution law of the working face by establishing a UDEC2D numerical model, combined with field borehole stress meter test results and theoretical calculations. Frid tested the variation law of electromagnetic radiation intensity under different coal-rock mechanical states in the field, and measured the decompression intensity of coal-rock using a resonant frequency of 100 kHz. Lin Baiquan et al. found that rock burst is directly related to the size of the decompression zone ahead of the roadway; the shorter the decompression zone, the greater the possibility of rock burst accidents[8-13].

Although some research results have been achieved on the stress distribution law of the coal body around the stope, due to the significant influence of mining intensity, overlying strata conditions, and coal seam gas geological conditions on the stress distribution of the gob-side, it is still difficult to accurately determine the stress distribution law of the gob-side coal body under specific mining conditions. Therefore, this paper takes the N2107 working face of Yuwu Coal Mine as an example, and adopts theoretical analysis, field monitoring, and microseismic data inversion to explore the stress distribution law and evolution characteristics of the gob-side coal body, in order to provide theoretical and technical support for safe and efficient coal mining.

## **2. THEORETICAL ANALYSIS OF STRESS DISTRIBUTION IN GOB-SIDE COAL BODY**

### **2.1. Theory of Mining-Induced Stress Distribution**

During underground mining operations in coal mines, the original stress equilibrium state inside the coal body is broken, causing the redistribution of internal stress in the coal body. In the initial period of mining activities, stress will form concentrated areas ahead of the stope and around the roadway operations. As mining operations proceed, the concentrated stress value will increase until it exceeds the yield limit of the coal body, and this part of the coal body will undergo yield deformation. Over time, the concentrated stress will transfer to the distance with the progress of mining.

The horizontal stress of the coal body in the goaf gradually increases with the depth of the coal body to the original stress; the tangential stress first rapidly increases to the peak and then slowly decreases to the original stress. After a period of time, decompression zones, stress concentration zones, and original stress zones will be formed around the mining operations. The three zones will continuously move forward with the advance of the working face. Because the stress field formed by mining is continuous and continuously transmitted forward in the form of stress waves, the ranges of the three zones remain roughly unchanged.

(1) Decompression zone: After the working face is mined, affected by concentrated stress, the edge coal body within a certain range is first "crushed," producing fractures, resulting in a significant reduction in the bearing capacity of the coal body, which can only bear loads lower than the original rock stress.

(2) Stress concentration zone: The stress concentration zone includes the plastic deformation zone and the elastic deformation zone. The boundary between the plastic deformation zone and the elastic deformation zone is the peak stress concentration. The coal body in the plastic deformation zone is under biaxial or even triaxial stress, while in the elastic deformation zone, the stress on the coal body has not reached the yield limit, and the coal body is in the elastic deformation stage. Therefore, in the stress concentration zone, the stress on the coal body first gradually increases to the peak stress and then gradually decreases.

(3) Original stress zone: The coal body is far from the goaf, not affected by mining disturbance, and the stress environment is stable. Therefore, the bearing state of the coal body in this zone basically remains unchanged.

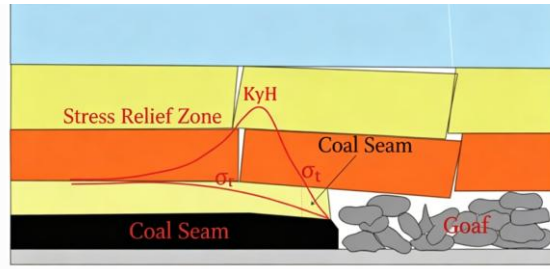


**Fig. 1** Schematic diagram of the three zones of coal-rock mass

## 2.2. Field Test

The N2107 working face of Yuwu Coal Industry is located in the east wing mining area of Yuwu Coal Industry, arranged in the north-south direction. To its west is the goaf of the N2106 working face. The belt roadway is 1298 m long, and the return airway is 1228 m long. The main mining seam is the No. 3 coal seam, with an average thickness of 6.5 m, an average dip angle of  $2^\circ$ , and the coal seam floor elevation of +460 to +490 m. The plan layout of the N2107 working face is shown in the figure below.

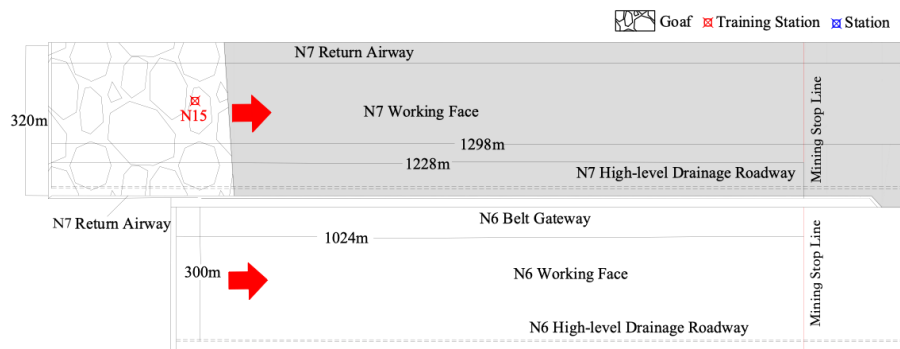


**Fig. 2** Mining plan of the 2107 working face

Stress meters were installed at intervals of 40 m ahead of the goaf using borehole stress meter installation monitoring. The borehole stress meter can better conform to the original stress of the coal body. With the deformation of the borehole caused by the stress change of the surrounding rock under the influence of dynamic pressure, the stress change transmitted by this deformation is received to achieve the purpose of continuous observation of the surrounding rock stress.

## 2.3. The color is more gorgeous

Microseismic waves are tiny vibrations caused by changes in the stress field of rock mass leading to rock fracture or fluid disturbance. These waves can be captured by high-precision monitoring equipment and used to analyze the dynamic changes of rock mass. This study adopts the surface microseismic monitoring method. The observation system is arranged according to the following two principles: (1) it should cover the entire study area, and the boundary of the observation system should be larger than the study area; (2) to minimize the recording error of microseismic events in the monitoring area, stations should be evenly distributed in the test area, and the interval should be greater than half of the monitoring depth. According to the above basic principles and the geological conditions of the test area, 24 monitoring stations were arranged on the N2107 working face, covering three adjacent working faces including N2107. The layout of microseismic monitoring equipment is shown in the figure below:

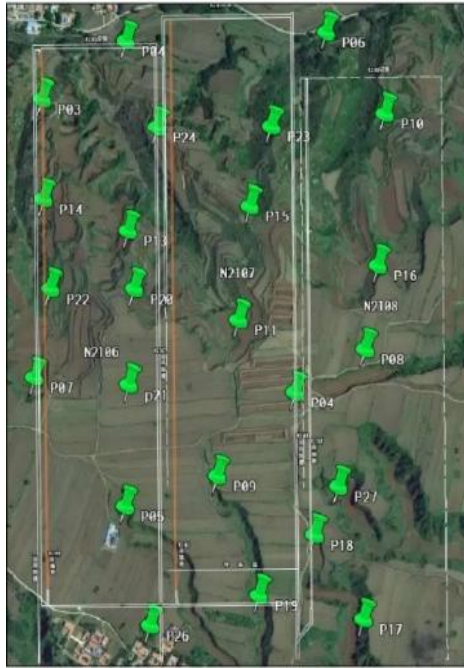


**Fig. 3** Layout of microseismic stations

The monitoring parameters of all microseismic monitoring equipment are: sampling frequency 15–1500 Hz, sensitivity 52 V/S. The collected microseismic data are uploaded to the cloud in real time through the 4G network for processing. Figure 4 shows the original signals received by different stations in the study area for the same microseismic event. It can be seen that the first arrival points are relatively obvious, and the data quality is relatively reliable.

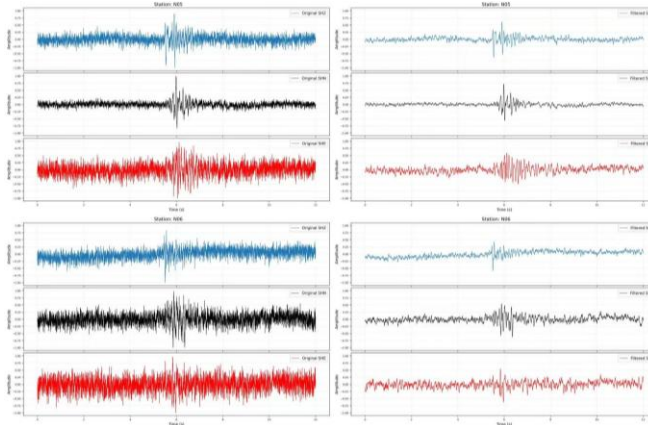


**Fig. 4** Original waveforms of microseismic events

### **3. SIMULATION OF STRESS DISTRIBUTION CHARACTERISTICS OF COAL ROADWAY HEADING FACE BASED ON MICROSEISMIC DATA**

#### **3.1. Monitoring Analysis of Borehole Stress Meters in Return Airway Coal Pillar**

The stress field formed by mining is continuous and continuously transmitted forward in the form of stress waves, so the ranges of the three zones remain roughly unchanged. Therefore, the monitoring results of stress meters were randomly selected, and the data collected by field stress meters were analyzed, where the value 0 is caused by equipment abnormality.

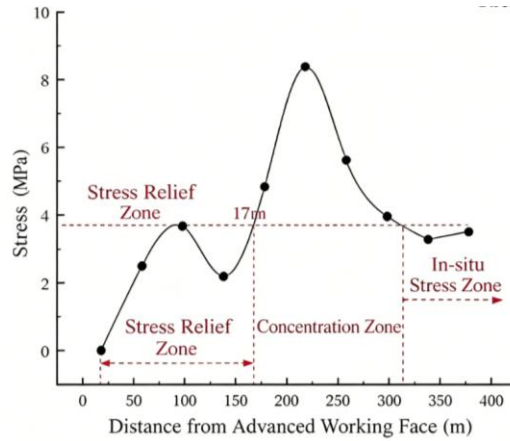


**Fig. 5** Monitoring data of stress meters at different positions

The measured results of the advanced mining-induced stress of the N2107 working face are shown in the above figures. The readings of the borehole stress meters began to rise at a distance of 150–190 m from the N2107 working face, indicating that the maximum influence range of stress concentration is about 190 m.

### 3.2. FLAC3D Numerical Simulation of Mining-Induced Stress Distribution

To accurately reveal the stress evolution law of the gob-side coal body of the N2107 working face, FLAC3D three-dimensional numerical simulation software was used to construct a stope-coal body coupling model. By simulating the dynamic distribution characteristics of coal body stress during the mining disturbance process, the stress zoning range and evolution law were clarified. Combined with the actual geological conditions of the N2107 working face of Yuwu Coal Mine, the model range fully covers the study area and the influence boundary. The core area of the N2107 working face and the gob-side coal body was subjected to grid encryption (grid size 5 m × 5 m × 3 m), and the grid size gradually increased in areas away from the core area (maximum grid size 10 m × 10 m × 8 m), with a total grid number of about 1.2 million, ensuring a balance between simulation accuracy and computational efficiency. The coal-rock medium adopts the Mohr-Coulomb constitutive model, which can better reflect the yield and failure characteristics of coal-rock under complex stress conditions and conforms to the engineering reality of mining-induced stress evolution in coal mines. The mechanical parameters of each rock layer and coal seam in the model are based on laboratory rock mechanics test results. The specific parameters are shown in Table 1, ensuring the rationality and reliability of the parameters.

**Table 1** Parameter values for mining-induced stress distribution calculation

Lithology	$\gamma$ (MN/m <sup>3</sup> )	Mining depth (m)	Friction angle $\varphi$ (°)	Cohesion $c$ (MPa)	Tensile strength $\sigma_T$ (MPa)	Compressive strength $\sigma_c$ (MPa)
Siltstone	0.026	552.20	36	3.0	3.10	107.1
Fine-grained mudstone	0.027	555.72	28	2.7	5.80	69.07
Siltstone	0.026	561.22	36	3.0	3.10	107.1
Mudstone	0.025	566.50	30	2.0	2.20	12.2
3# Coal	0.015	568.00	37	1.8	1.40	13.9
Mudstone	0.024	574.50	42	2.0	2.20	12.2

Fixed displacement constraints were applied at the bottom of the model (displacement in x, y, and z directions is 0); horizontal displacement constraints were applied on the four sides (displacement in x and y directions is 0), allowing vertical free deformation; a uniformly distributed load was applied at the top to simulate the self-weight of the overlying strata, and the load magnitude was calculated according to  $\gamma H$  to ensure consistency with the actual in-situ stress environment. The initial in-situ stress field was assigned according to the gravity stress field.

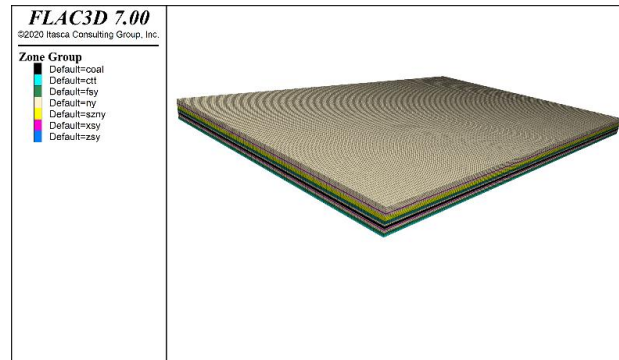


**Fig. 6** FLAC3D model diagram

Through FLAC3D simulation, the stress distribution nephograms and stress curves of the gob-side coal body of the N2107 working face at different mining stages were obtained. Combined with the numerical characteristics of stress, the gob-side coal body can still be divided into three characteristic zones: the decompression zone, the stress concentration zone, and the original stress zone. The distribution and evolution laws of each zone are as follows:

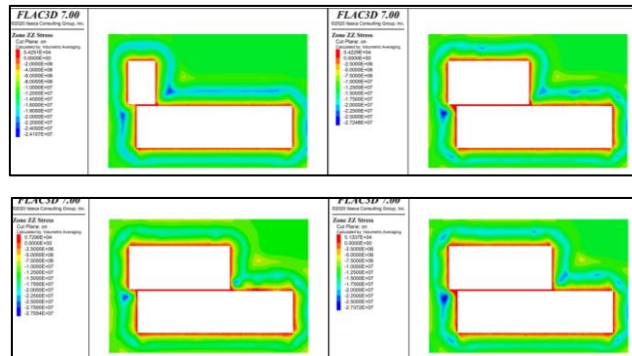


**Fig. 7** Plane stress nephograms at different mining positions

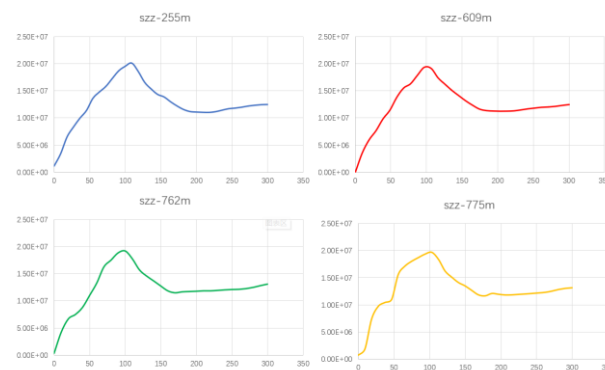


**Fig. 8** Stress curves at different mining positions

It can be seen that the FLAC3D simulation captures the continuous characteristics of the stress field. The three zones move forward synchronously with the advance of the working face in the form of stress waves, and the zone ranges remain basically stable during the mining process, which is

consistent with the stress field transmission law of theoretical analysis. The decompression zone range is about 100 m.

### 3.3. b-Value Inversion Based on the Gutenberg-Richter Formula

In 1941, Gutenberg and Richter found through the study of a large amount of earthquake data that there is a power-law distribution relationship between earthquake magnitude  $M$  and the number of earthquakes  $N$  with magnitude greater than  $M$ , namely the G-R relationship:

$$\lg N = a - bM \quad (1)$$

Where,  $a$  and  $b$  are constants and are important parameters describing the frequency-magnitude distribution characteristics of earthquakes in a seismic zone. They can be calculated from seismic data through formulas. Among them,  $a$  reflects the average level of seismic activity;  $b$  reflects the proportional relationship between large and small magnitudes. In the field of earthquake prediction, studies have found that before large earthquakes, certain magnitude classes of earthquakes in the focal area and nearby areas often increase or decrease, leading to an imbalance in the proportion of large and small earthquakes and an abnormal phenomenon of decreasing b-value. In addition, the increase in regional stress accumulation level is a necessary condition for the occurrence of large earthquakes. Therefore, it is believed that the b-value reflects the crustal stress state, and the two are inversely proportional.

The N2107 working face began mining on November 20, 2023. The microseismic equipment has been operating stably for a long time. Since 2024, a total of 80,698 effective microseismic events have been collected.

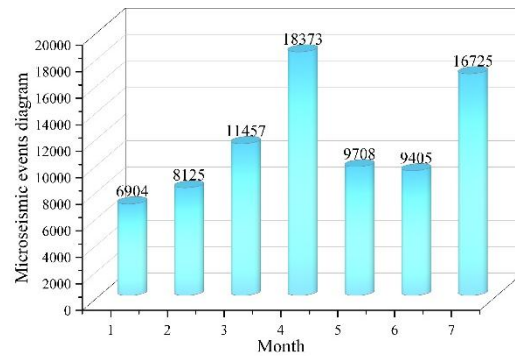


**Fig. 9** Frequency diagram of microseismic events

In this paper, the b-value of the microseismic events collected from the working face was calculated by month. According to the relationship between rock structure and b-value, it is known that areas with higher b-values correspond to lower stress. The study area was divided into grids of  $100\text{ m} \times 100\text{ m}$ . The microseismic events within each grid were statistically analyzed and the b-value was calculated. The calculated b-value was used as the seismic b-value at that grid point. Then, the b-values of all grid points were interpolated to draw the b-value distribution nephogram, converting the distribution of discrete microseismic events into a continuous formation stress distribution. The b-value nephograms from January to July are shown below:

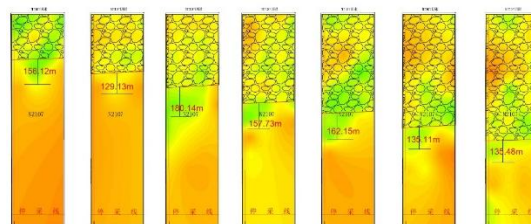


**Fig. 10** b-value distribution nephograms of the N2107 working face from January to July

It can be seen that during the roadway mining process, there is obvious stress stratification in the gob-side coal seam. There is a low-stress area of about 150 m ahead of the goaf.

## 4. RESULTS AND DISCUSSION

(1) The influence range of stress concentration of the mining working face is mainly controlled by the strength of the coal-rock mass and the fracture and activity law of the main roof above the working face. Combined with the FLAC3D numerical simulation, field microseismic data inversion, and stress meter monitoring results of the N2107 working face, it is known that the peak of the advanced abutment stress of the N2107 working face is located about 150 m from the gob-side of the working face. The results of the three methods verify each other, improving the credibility of the stress distribution law.

(2) The microseismic b-value can be used to analyze the crustal stress state. By converting discrete microseismic events into continuous reservoir stress conditions, it has important guiding significance for confirming the gob-side decompression zone and preventing rock burst.

(3) Based on the determined stress zoning parameters, in actual mining, pressure-relief boreholes or directional hydraulic fracturing measures can be arranged in advance in the stress concentration peak area (120–180 m from the gob-side) to reduce the degree of stress accumulation; support parameters can be optimized in the decompression zone (range from the working face coal wall to 35 m from the gob-side). Combined with real-time microseismic b-value monitoring data, when the b-value in a specific area shows a continuous decreasing trend, the risk of stress concentration should be warned in time and the mining rhythm should be adjusted. This can effectively improve the guarantee capability for safe and efficient mining of deep coal resources.

## REFERENCES

- [1] Cheng, Q. Y., Sun, C. X., Zhang, X. X., et al. (2004). Short-term load forecasting model and method for power system based on complementation of neural network and fuzzy logic. *Transactions of China Electrotechnical Society*, 19(10), 53–58.
- [2] Fang, F. (2011). *Research on power load forecasting based on improved BP neural network* (Master's thesis). Harbin Institute of Technology.
- [3] Amjady, N. Short-term hourly load forecasting using time series modeling with peak load estimation capability.
- [4] Xue, C., Zhao, J. F., & Wang, G. S. (2011). Study on advanced abutment pressure distribution law of working face in Dongqu Coal Mine. *Coal Science and Technology*, 39(6), 9–11.
- [5] Lin, B. Q., Zhou, S. N., & Zhang, R. G. (1993). Coal roadway decompression zone and its application in the prediction of coal and gas outburst hazard. *Journal of China University of Mining & Technology*, (4), 47–55.
- [6] Wang, M. K. (2020). *Study on the width of decompression zone and gas drainage zone in the same coal seam of goaf in Xintun Mine* (Master's thesis). Henan Polytechnic University.
- [7] Qian, M. G., & Xu, J. L. (2019). Coal mining and rock strata movement. *Journal of China Coal Society*, 44(04), 973–984. <https://doi.org/10.13225/j.cnki.jccs.2019.0337>
- [8] Xue, C., Zhao, J. F., & Wang, G. S. (2011). Study on advanced abutment pressure distribution law of working face in Dongqu Coal Mine. *Coal Science and Technology*, 39(06), 9–11. <https://doi.org/10.13199/j.cst.2011.06.15.xuech.011>
- [9] Frid, V. (1997). Rockburst hazard forecast by electromagnetic radiation excited by rock fracture. *Rock Mechanics & Rock Engineering*, 30(4), 229–236.
- [10] Lin, B. Q., Zhou, S. N., & Zhang, R. G. (1993). Coal roadway decompression zone and its application in the prediction of coal and gas outburst hazard. *Journal of China University of Mining & Technology*, (04), 47–55.
- [11] Li, X. M., Xu, L., & Meng, Z. W. (2025). Simulation study on surrounding rock stability of mining roadway under different stress environments. *Shandong Coal Science and Technology*, 43(11), 1–5+11.

- [12] E, Z. K., & Yang, X. L. (2025). Deformation and failure mechanism and control measures of roadway under repeated mining in shallow buried thick coal seam. *Energy New Observation*, (11), 39–41.
- [13] Kang, H. P., & Gao, F. Q. (2024). Mining-induced stress evolution and surrounding rock control in coal mines. *Chinese Journal of Rock Mechanics and Engineering*, 43(01), 1–40. <https://doi.org/10.13722/j.cnki.jrme.2023.1055>
- [14] Jing, G. C., Cao, A. Y., Dou, L. M., et al. (2017). Focal mechanism of rock burst in folded structure area of coal mine. *Journal of China Coal Society*, 42(01), 203–211. <https://doi.org/10.13225/j.cnki.jccs.2016.0951>
- [15] Kang, H. P. (2013). Stress distribution characteristics and roadway surrounding rock control technology in deep coal mines. *Coal Science and Technology*, 41(09), 12–17. <https://doi.org/10.13199/j.cnki.cst.2013.09.007>
- [16] Kang, H. P., Wu, Z. G., Gao, F. Q., et al. (2012). Influence of geological structures on in-situ stress distribution in underground coal mines. *Chinese Journal of Rock Mechanics and Engineering*, 31(S1), 2674–2680.